Asociación Argentina
de Mecánica Computacional

Mecánica Computacional Vol XXXV, págs. 123-134 (artículo completo)
Martín I. Idiart, Ana E. Scarabino y Mario A. Storti (Eds.)
La Plata, 7-10 Noviembre 2017

NATURAL CONVECTION IN A REPRESENTATIVE SECTION OF AN ONAN DISTRIBUTION TRANSFORMER

Paola A. Córdoba[a,c], **Enzo A. Dari**[a,c] **and Nicolás Silin**[b,c]

[a]*Departamento de Mecánica Computacional*

[b]*Grupo de Materiales Nucleares*

[c]*Centro Atómico Bariloche-CNEA, Instituto Balseiro-UNCUYO, CONICET, Av. Bustillo 9500, S.C. de Bariloche, Río Negro, Argentina*

Keywords: Natural Convection, transformer cooling, Finite Element Method, 3D Modeling.

Abstract. We present a 3D numerical modeling of an ONAN distribution transformer. We found that the 3D problem of natural convection in this thermohidraulic device can be studied by a numerical model that represents a 3D slice of an ONAN distribution transformer. The numerical study was carried out by applying the Finite Element Method to solve the 3D Navier-Stokes and heat equations using the in-house developed Par-GPFEP code. We compared the present results with those of other authors who used a similar approach with some differences in the solution method and in the simplifications considered. Also we compared the numerical temperature distribution with thermographies presented in a heating test performed in an ONAN transformer provided by Tubos Trans Electric S.A. The numerical results are also compared with velocity fields measurements taken in an experimental device that was built to simulate a representative slice of the transformer of interest. A PIV setup was used to obtain the flow velocity field. We found reasonable agreement between numerical and the preliminary experimental results, showing stratified temperature distributions and similar flow patterns in the studied region.

1 INTRODUCTION

The main motivation of this work is the analysis of the flow pattern and heat transfer in an ONAN (Oil Natural Air Natural) type power transformer. Fig. 1 shows the general parts of a 1000 KVA distribution transformer. In the design of interest, fins are integral part of the walls being manufactured by folding a metal sheet (see Fig. 1-c). The resulting flexibility of the walls allows to compensate the volume changes of the oil without an expansion tank. These type of transformers are oil filled. This oil acts both as electrical insulator and as coolant fluid, maintaining the temperature of electrical components within acceptable limits. Transformers produce heat in the ferromagnetic core and in the coils due to unavoidable power losses. The oil is heated by the core and the coils and circulates to the hollow fins, where it is cooled down. The fins provide an exchange surface with the air and heat is transferred, again by natural convection, therefore the ONAN denomination.

There are both, country specific regulations (In Argentina we have the IRAM 2018:1995) and international standards (IEC 354:1991; IEC 60076–7:2005) that define the allowable operation conditions for these devices. These regulations give mathematical models for the calculation of operating temperatures in the transformer, in particular the temperature of the hottest spot of the winding. The IEC 354:1991 also suggest a series of working temperature boundaries to avoid premature degradation of the oil or the transformer materials. In spite of these regulations it is still up to the manufacturer to achieve a design that satisfies these limits while minimizing the size and cost of the transformer. This is a rather challenging task that normally involves trial and error and ends up with varying degrees of over dimensioning.

This problem has been widely studied from the computational point of view. The CFD approach allows not only to predict the hot spot temperature but also the temperature distribution and the flow pattern. The knowledge of the fluid field inside transformer can then be used to optimize its cooling. El Wakil et al. (2006); Torriano et al. (2012, 2010), among others, studied the thermal distribution and flow pattern in a disc-type power transformer by CFD modeling of the cooling channels in the winding. Regarding the ONAN type transformers, and due to the complexity of the problem, to model all the details of the transformer structure is still computationally expensive. Thus, depending on the researcher, several geometric simplifications are used, (Gastelurrutia et al., 2011a,b; Tsili et al., 2012; Córdoba, 2016). Tsili et al. (2012), built two separated models, one for the solid active parts of the transformer, i.e. winding and core, and one for the oil tank. Then they coupled the results of the thermal solver with the CFD solver in an iterative process obtaining the temperature distribution. They point out that an experimental validation of their oil local velocity results is quite difficult.

In this work we present a 3D modeling of a commercial transformer of 1000 KVA (Tubos Trans Electric S.A. 1000 KVA Standard Distribution Transformer). In this model, the oil flow domain is reduced to a slice of the complete transformer. We compared the present results with those of Gastelurrutia et al. (2011a) who used a similar approach with some differences in the solution method and in the simplifications considered. Also we compared the numerical temperature distribution with thermographies presented in the Heating test No.7076–08 performed in an ONAN transformer provided by Tubos Trans Electric S.A. We found a satisfactory agreement between our numerical results and those of Gastelurrutia et al. (2011a) and the thermographies of the Heating test No.7076–08. Then we present an additional validation of the numerical results with preliminary measurements of the flow field in an experimental device that simulates a representative slice of an ONAN distribution transformer.

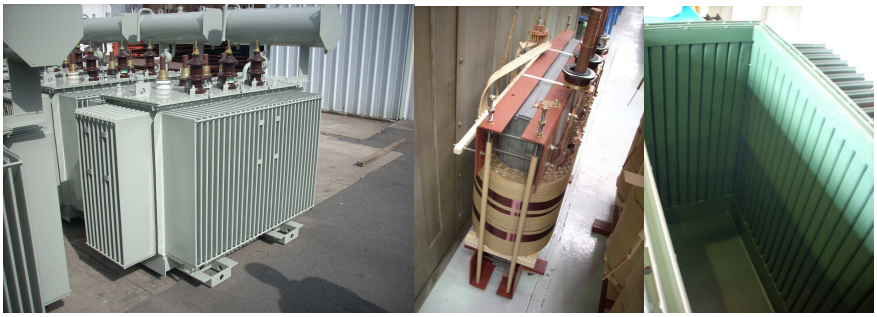

(a) (b) (c)

Figure 1: general parts of a 1000 KVA ONAN distribution transformer. (a) External view, (b) core and winding, (c) tank.

2 3D MODELLING

2.1 General aspects

Due to the high computational cost that would imply a simulation of the transformer full geometry, we model a Representative Section (RS). This section is constructed in order to reproduce the basic phenomenology of cooling process. This approach to the problem has already been used by others authors (see Gastelurrutia et al. (2011a)) as a way of reducing computational costs.

Fig. 2 shows the RS scheme. The RS is defined using the following criteria: the fin geometry and the tank height are exactly modeled as well as the distance between the symmetry plane passing through the three coils and the tank vertical walls.

The vertical dimensions are important to model adequately the buoyancy force, while the distance between the fins and the symmetry plane determines the space available for possible flow recirculation inside the tank, without going through the fins. The RS width is defined in order to reproduce the total tank volume, thus the coolant thermal inertia is accurately modeled. A symmetry boundary condition is imposed in the normal direction to the fins. Then, the problem is equivalent to having infinite sections side by side to each other.

The transformer ferromagnetic core was considered as a rectangular region, located in the central region of the transformer tank, with a volume equivalent to the real core one. Thus, the SR has a portion of the core as shown in Fig. 2. With this geometric simplification the volume subtracted from the tank by the presence of the ferromagnetic core is reproduced. The heat generated in the winding is modeled by defining a homogeneously heated region with a height equal to original coils height and a thickness such that original volume it is conserved. With this simplification we seek to simulate the buoyant force due to the energy per unit volume supplied to the system by the copper losses.

According to the described criteria, the geometry shown in the figure 2 is obtained. The fin is a parallelepiped with dimensions of 270mm x 7mm x 900mm. The total volume of transformer tank (without the fins) is 1060mm x 1330mm x 480mm. Keeping the height in 1060mm and the depth in 240mm from the vertical plane of symmetry, the width of the RS tank is 33.25mm. Thus, the RS occupies a fraction equal to 1/80 of the total volume of the original transformer. Note that the actual separation between fins is 45 mm, however, the presence of fins on the short sides of the transformer tank implies that the average separation between fins is smaller in the model of RS.

The total volume of the core ferromagnetic material is 128 liters. For a geometrical simplicity

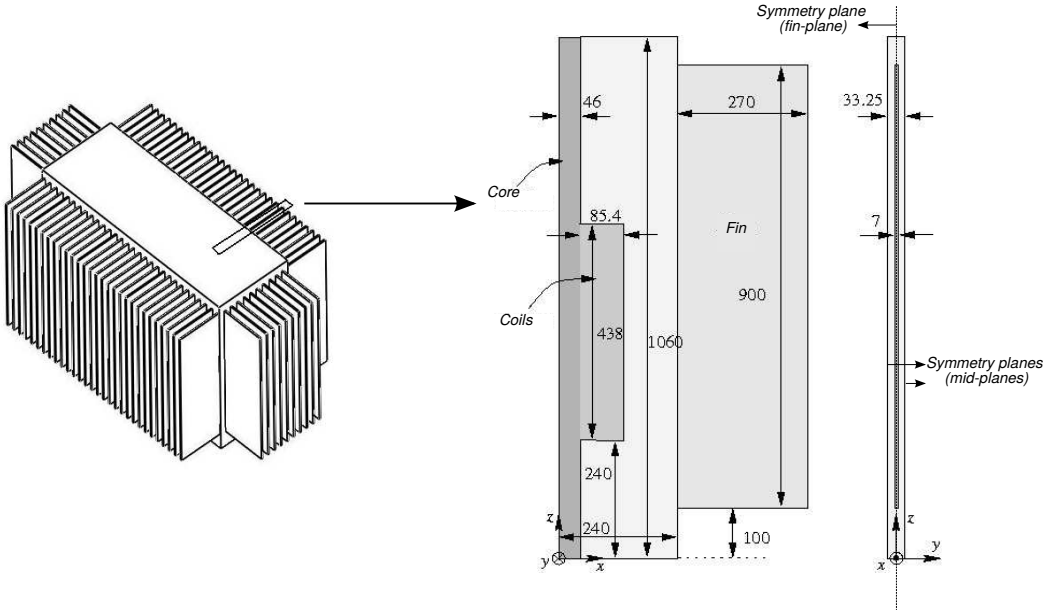

Figure 2: Transformer Representative Section.

this volume was uniformly distributed along the tank height, resulting in a rectangular zone of 33.25mm x 46mm x 1060mm. With this simplification it is possible to remove from the simulation domain the core zone introducing an appropriate thermal boundary condition.

Each of the three coils forming the winding transformer has a height of 438mm, an inner radius of 118mm and an outer radius of 195mm. This total volume is 99.5 liters and it was distributed in 80 RS forming a region of 85.4mm x 33.25mm x 438 mm within each RS.

2.2 Governing Equations

The flow in the RS cavity is governed by the incompressible Navier-Stokes and energy equations, where the Boussinesq approximation is considered. The dimensional form of this equations can be expressed as

$$\rho_0[\partial_t u + (u\cdot\nabla)u] - \nabla\cdot[2\mu(T)\nabla^s u] + \nabla p = f, \tag{1}$$

$$\nabla\cdot u = 0, \tag{2}$$

$$\rho_0 Cp[\partial_t T + (u\cdot\nabla)T] - k\nabla^2 T = S, \tag{3}$$

$in \quad \Omega, \quad t \in (0,T)$ where u is the velocity vector with components u_x, u_y and u_z. $f = \rho_0 g[1-\beta(T-T_0)] - \rho_0 C_f u$, where the first term is the buoyancy force, being ρ_0 the oil density at the temperature T_0. The buoyancy force is written in this form to avoid the density evaluation at the local temperature. The second term is the Darcy's term that constitutes a hydrodynamic simplification of the transformer coils, considering it as a porous region mainly affected by a friction factor C_f. $\nabla^s u = \frac{1}{2}[(\nabla u) + (\nabla u)^{\mathbf{T}}]$ is the symmetric gradient operator. Ω is the n -dimensional domain where the problem will be solved in the time interval $(0,T)$. The working fluid is a mineral napthenic YPF64 oil with viscosity μ. One of the characteristics of this oil is the viscosity dependence on temperature. A complete characterization of this oil can be found in Cordoba et al. (2015). The function $\mu(T)$ considered in this model can also be found in Cordoba et al. (2015). k and Cp are the thermal conductivity and the specific heat respectively

of the working fluid. The physical properties of the mineral oil used in this model can be found in Table 1.

Physical property		Value
Density (kg/m^3)	ρ	880
Thermal conductivity (W/mK)	k	0.126
Specific Heat (J/kgK)	C_p	1860
Thermal diffusivity (m^2/s)	α	7.7×10^{-8}
Thermal expansion coefficient (K^{-1})	β	0.00075

Table 1: Fluid properties of the YPF64 oil.

According to data provided by Tubos Trans Electric S.A. from dissipation measurements of a transformer in no-load operation, the power loss in the core accounts for 1740 W while the copper losses at full-load operation account for 10816 W. We used the assumption that the heat generated by the power loss in the core is uniformly distributed over the whole core surface. The RS comprises one fin of a total number of 80 and therefore we have taken a heat flux through the surface in contact with the core, with dimensions 33.25mm x 1060mm, of $q'' = 617.1W/m^2$. Thus, the heating due to the power loss in the core was modeled as a Neumman boundary condition corresponding to a constant heat flux thermal boundary condition at the surface in contact with the core.

The copper losses were included in the model as a volumetric heat source (S in the eq. 3) at the winding region. The resulting heating power due to the copper losses was set to 135.2 W.

For the energy equation, the symmetry plane and the insulated walls have Neumman boundary conditions $\frac{\partial T}{\partial \hat{n}} = 0$, while the cooling of the fins due to the air natural convection is modeled through Neumman boundary conditions, i.e. convection conditions: $k\frac{\partial T}{\partial \hat{n}} = \overline{h}(T_s - T_a)$. These conditions depend of the surface temperature T_s of the cavity walls and the convection coefficient $\overline{h}$. These convection coefficients were considered constants on each horizontal wall and they were estimated by using convective correlations from bibliography (Incropera and DeWitt, 1996). For the vertical fin walls we used the Nusselt number correlation proposed by Gastelurrutia et al. (2011a), and the Nusselt number definition (4) and we estimated a convection coefficient that depends of the temperature $T_s(z)$ at the z coordinate. Thus, the convection coefficient is given by relation (5), where T_a is the ambient temperature.

$$\overline{h} = \frac{k_a \overline{Nu}}{d}, \tag{4}$$

$$\overline{h}(z)_{finwalls} = 4.1254(T_s(z) - T_a)^{0.2364} \tag{5}$$

where d is the separation between the fins and k_a is the thermal conductivity of the air. The air properties were evaluated at 30 °C. The convection coefficients used in the model are shown in Table 2.

We use the no-slip boundary conditions for velocity, i.e. $u_x = u_y = u_z = 0$ at all walls, except in the symmetry plane where the slip boundary condition was used, i.e. $\frac{\partial u_x}{\partial y} = \frac{\partial u_z}{\partial y} = u_y = 0$.

Zone	$\overline{h}$
Fin walls, tank vertical wall	$\overline{h}(z)_{finwalls}$
Horizontal top walls	1.99
Horizontal bottom walls	1.00

Table 2: Convection coefficients used in the code. The convection coefficient is expressed in (W/m^{2}K).

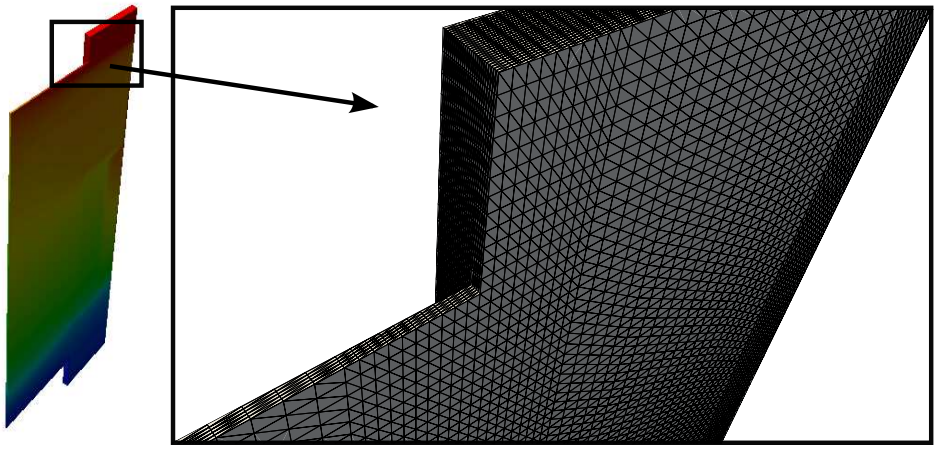

Figure 3: Non-uniform structured mesh with tetrahedral elements used to model the RS.

2.3 Solution Method

The equations (1)-(3) have been solved by the Finite Element Method. In this work we use the Standard Galerkin approximation with the addition of stabilizer terms according to the SUPG method (Codina, 1998). The variational formulation of this problem can be found in Cordoba et al. (2015).

2.4 Grid characteristics

Based on the results obtained in a previous experimental work (Córdoba, 2016), the thickness of the boundary layer in the region of maximum velocity is about 3×10^{-2}m. Taken into account this length scale, a non-uniform grid, as shown in Fig. 3, was built. This structured mesh is composed by 1576680 elements and 286833 nodes. The simulation domain corresponds to half of the RS due to the symmetry of the problem. The grid dimensions are the same as those of geometry detailed in Fig. 2. The mesh is non-uniform in the x-direction, with a minimal spatial resolution near the wall of 3×10^{-3} m, and uniform in the remaining directions. The grid spacing in the y and z-directions are 7×10^{-4} m and 5×10^{-3} m respectively.

3 EXPERIMENTAL SETUP AND MEASUREMENT METHOD

The Experimental Device (ED) was build in order to simulate a representative section of an ONAN (Oil Natural - Air Natural) 1000 KVA distribution transformer encompassing two fins. In the ED the heating by cooper losses in the transformer winding are simulated by an electrical heating element. A double glass window allows visual access for flow visualization and PIV capture. To achieve thermal similarity on the air natural convection side, the two fins were shielded with polystyrene foam boards. Fins and boards form three air channels as sketched in

Fig. 4 (Top view). This figure also shows the device dimensions and the reference coordinate system. The heating element consists of an aluminum structure that was built with seven arrays of aluminum vertical plates 0.365 m high.

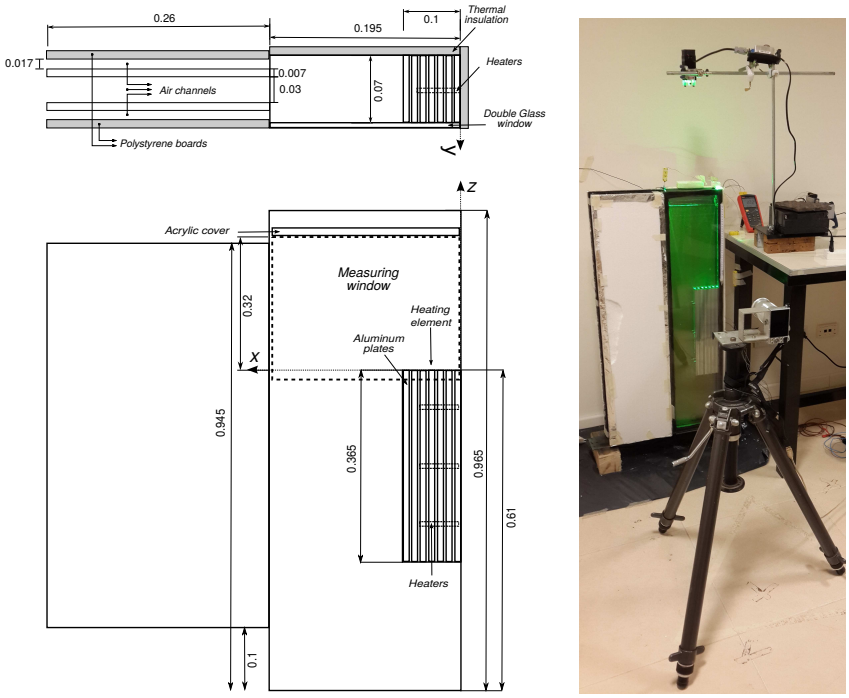

Figure 4: Schematic of the experimental device. (a) (Bottom) Cavity front view, (Top) Cavity top view. (b) Experimental array and PIV setup.

Three Watlow FIREROD cartridge electrical heaters, with a diameter of 6.5 mm and a heating length of 50 mm each, were inserted perpendicular to these walls. These heaters were uniformly distributed along the vertical and in a good thermal contact with the aluminum plates.

The core losses account for the 20% of the losses, here we will focus on copper losses that account for 80% the total power loss of the transformer.

The test section comprises two fins of a total number of 80 and therefore we have taken a heating power of 270.4 W. The tank is open at the top to allow for easy access, oil manipulation and cleaning. The cavity is completely filled with mineral oil YPF64. Once the ED is filled with oil, a floating acrylic cover is introduced. This cover supplies a non-slip boundary condition while allowing for volumetric expansion of the oil.

Ideally we would like to have a boundary condition of symmetry at half the air channel width from the external fins. This is not possible in an experimental device, we decided in turn to generate air gaps parallel to the external walls of the fins and to have these walls reflective and thermally isolated. This was achieved by isolating the symmetry boundary walls. The fins, on the other hand, were shielded with aluminized polystyrene foam boards but allowing a channel for the air to flow (see Fig. 4 (a: top view)), thus retaining air natural convection conditions.

We used planar Particle Image Velocimetry (PIV) to obtain the velocity fields. We took advantage of the low velocities to be measured, approximately $\sim 10^{-2}$m/s, and designed an inexpensive PIV setup as shown in 4 (b). The images where captured by means of a Nikon 1 J5 digital camera, capturing 20 frames per second at a resolution of 20 Mpixel. For each flow field snapshot a burst of 20 consecutive frames were acquired and processed, obtaining 19 velocity

fields, which allowed reducing uncertainty. In this setup the illumination plane was generated by a continuous green laser with a nominal power of 400 mW and a wave length of 532 nm, and a Powell cylindrical lens with a fan angle of 30° to expand the laser. This plane was alternatively placed at two different offsets from the double glass window at $y = 0.0$ m (mid-plane) and at $y = 0.0175$ m (fin-plane).

SPHERICEL® hollow glass particles 10 μm in diameter, with a density of 1.01 g/cm^3, were used as flow tracers. When this particles are illuminated the scattered light is recorded by the digital camera focusing on the laser illumination plane (see Fig. 4 (b)) in the measuring window (see Fig. 4 (a) Front view). We decided to limit the flow field measurements to the upper region of the test section, which is the area where the strongest convective flow takes place.

4 RESULTS

4.1 Numerical results

In this section we present the numerical results obtained with this model and we compared the present numerical results with the numerical results of Gastelurrutia et al. (2011a) and the thermographies of the Heating test No.7076–08.

The velocity and temperature fields obtained once the system has achieved the steady state, are shown in Fig. 5 and Fig. 6, respectively. In these figures we present the flow and temperature fields at the symmetry planes of the simulation domain. These symmetry planes are located at $y = -0.016625$m and $y = 0$m (from now on we will call these planes: mid-plane and fin-plane respectively) (see $\sim$ Fig. 2).

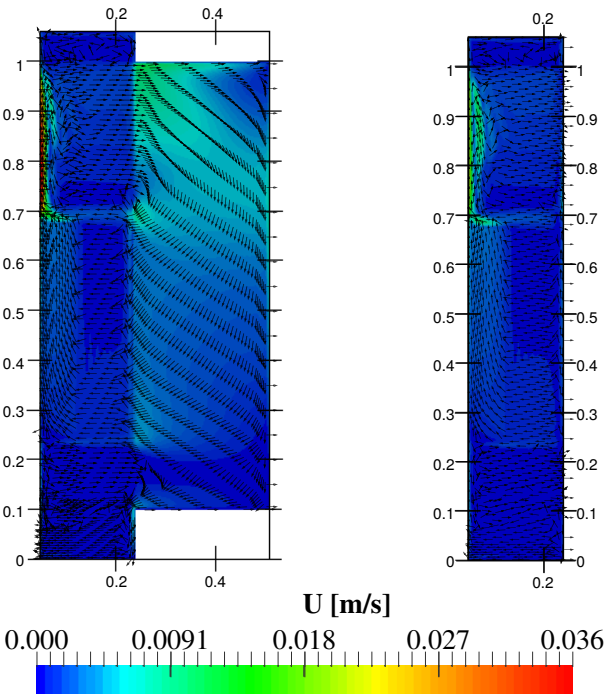

Figure 5: Velocity fields obtained from simulations at different planes. (left) fin-plane (right) mid-plane. The arrows were not scaled with the velocity vectors magnitude.

The velocity fields at the left side of this figure show a rising plume that arises from the heating region. This plume contracts rapidly after leaving the heating region and attaches to the vertical wall on the left side of the simulation domain corresponding to the surface in contact

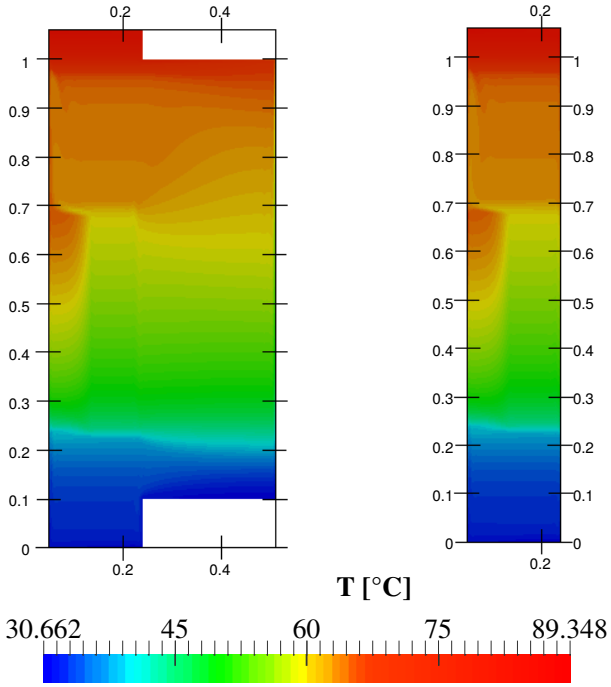

Figure 6: Temperature fields obtained from simulations at different planes. (left) fin-plane (right) mid-plane.

with the core. The fin-plane (see ∼ Fig. 5 (left)) shows that most of the main flow transported by the rising plume enters to the hollow fin, where it is accelerated due to the sudden contraction of the tank. This main flow is deflected downward due to the presence of the left vertical wall at the mid-plane as we can see in Fig. 5 (right). The velocity fields show two significant horizontal flows that arrive to the inlet and outlet of the heating region, coming from the fin, in the case of the fin-plane and coming from the downward flow in the case of the mid-plane. It can also be noted that higher velocities are only found close to the wall in contact with the core at the outlet of the heating region, while in the remaining zones, velocities are one order of magnitude lower.

We can also observe that the remaining portion of the flow transported by the rising plume generates a stagnation region of low velocities and high temperatures at the upper part of the tank due to the low mixing in this region. The temperature fields of the Fig. 6 show a stratified thermal distribution. The higher temperatures are presented in the heating region and in the upper part of the tank and fin.

The temperature and velocity fields obtained in present work are in good agreement with the predictions of the numerical model of Gastelurrutia et al. (2011a) and Córdoba (2016) and the thermographies of the Heating test No.7076–08.

It can be noted that the flow field presented by Gastelurrutia et al. (2011a) exhibits similar characteristics: the two horizontal flows coming from the fin at the inlet and outlet of the heating region, the rising plume at the outlet of the heating region, and low velocities mainly in the remaining regions of the transformer. It should be noted that the velocity and temperature values obtained with the present numerical model are in good agreement with the numerical results of Gastelurrutia et al. (2011a).

On the other hand, Fig. 7 shows a thermography of an ONAN distribution transformer as the one studied in present work, obtained from the Heating test No.7076–08. This heating test was realized according to the national standard IRAM 2018:1995. This thermography was obtained

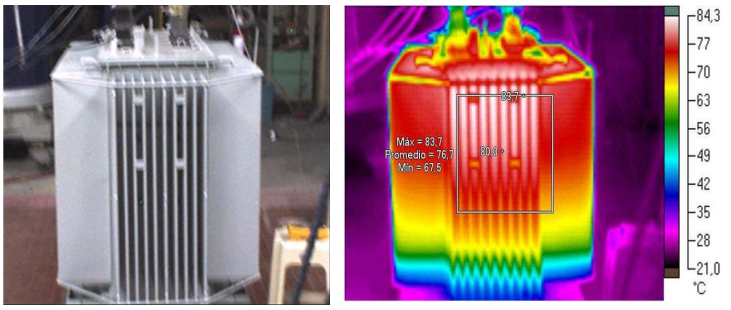

Figure 7: Thermography of an ONAN distribution transformer presented in the Heating test No.7076–08.

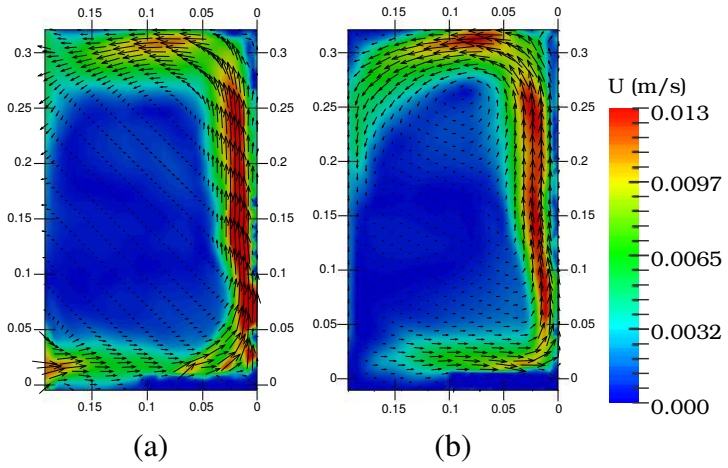

Figure 8: Experimental velocity fields measured at two planes of the ED. (a) fin-plane, (b) mid-plane.

at steady state and exhibits a similar temperature distribution respect to the present numerical results.

4.2 Preliminary experimental measurements

In this section we show a comparison between the numerical and the preliminary flow field measurements. The velocity fields obtained from the two measurement planes, once the ED has achieved the steady state, are shown in Fig. 8. The velocity field at the left side from this figure was measured at the cavity mid-plane while the one at right side corresponds to the fin plane.

We can observe similar flow field characteristics to those obtained numerically with the RS model. It should be noted that, as a symmetry boundary condition in the lateral vertical walls of the tank cannot be achieved, the numerical model was modified to replicate the experimental device. This means that this numerical simulation applies no slip boundary conditions to the aforementioned walls. We only considered the volumetric heating source at the heating region, and the geometry of the tank was modified in order to equalize it to the experimental device.

The numerical results obtained with these modifications are presented in Fig. 9. The flow fields shown in this figure, correspond to slices of the numerical solution at the fin-plane (see Fig. 9 (left)) and mid-plane (see Fig. 9 (right)) of the 3D simulation domain. We also identified on both planes the equivalent region of the selected measuring windows. It is noteworthy that both numerical and experimental flow patterns are in good agreement. We can conclude then that the simplifications considered in the RS model are suitable to reproduce the oil natural convection of an ONAN distribution transformer.

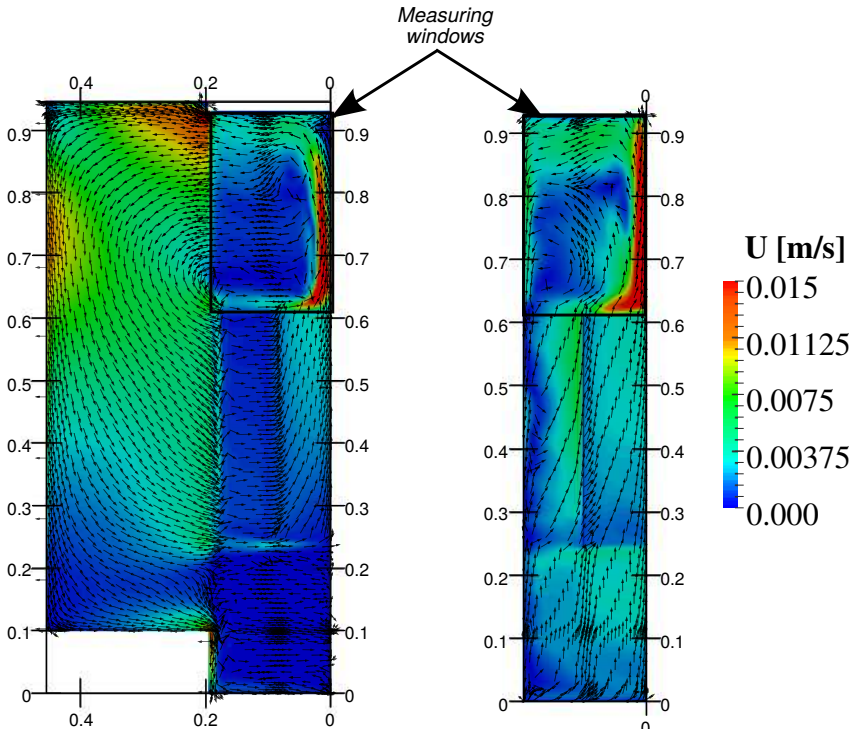

Figure 9: Velocity fields obtained from the modified numerical model. (left) fin-plane (right) mid-plane. The arrows were not scaled with the velocity vectors magnitude.

5 CONCLUSIONS

The present numerical modeling provides the basic flow patterns and temperature distribution in an ONAN transformer. The agreement of present results with the numerical results of Gastelurrutia et al. (2011a) and the Heating test No.7076–08 performed in an ONAN distribution transformer, as well as, the experimental validation of the numerical model, shows that the simplifications considered in present modeling are suitable to simulate the natural convection in these thermohidraulic devices. The flow inside the transformer is characterized by two horizontal flows coming from the fin at the inlet and outlet of the heating region, the rising plume at the outlet of the heating region, and low velocities in the remaining regions of the transformer. The present results may be used as reference to optimize the design of this device.

REFERENCES

Codina R. Comparison of some finite element methods for solving the diffusion-convection-reaction equation. *Computer Methods in Applied Mechanics and Engineering*, 156(1–4):185 – 210, 1998.

Córdoba P. *Estudio Numérico y Experimental para la optimización Termo-Fluido-Dinámica de transformadores de distribución tipo ONAN*. Ph.D. thesis, 2016.

Cordoba P.A., Silin N., and Dari E.A. Natural convection in a cubical cavity filled with a fluid showing temperature-dependent viscosity. *International Journal of Thermal Science*, 98:255–265, 2015.

El Wakil N., Chereches N., and Padet J. Numerical study of heat transfer and fluid flow in a power transformer. *International Journal of Thermal Sciences*, 45(6):615 – 626, 2006.

Gastelurrutia J., Ramos J.C., and Larraona G.S. Numerical modelling of natural convection of oil inside distribution transformers. *Applied Thermal Engineering*, 31(4):493–505, 2011a.

Gastelurrutia J., Ramos J.C., Rivas A., Larraona G.S., Izagirre J., and del Río L. Zonal thermal model of distribution transformer cooling. *Applied Thermal Engineering*, 31(17-18):4024 – 4035, 2011b.

Heating test No.7076–08. Informe de ensayo No. 7076–08. Technical report, Laboratorio de Alta Tension–F.C.E.F y Nat. – UNC, 2008.

IEC 354:1991. IEC 354:1991, Loading Guide for Oil-Immersed Power Transformers. Standard, International Electrotechnical Commission, 1991.

IEC 60076–7:2005. IEC 60076–7:2005, Loading Guide for Oil-Immersed Power Transformers. Standard, International Electrotechnical Commission, 2005.

Incropera F. and DeWitt D. *Fundamentals of Heat and Mass Transfer*. John Wiley and Sons, 1996.

IRAM 2018:1995. IRAM 2018:1995, Transformadores de potencia, ensayos de calentamiento. Standard, Instituto Argentino de Normalización y Certificación, 1995.

Torriano F., Chaaban M., and Picher P. Numerical study of parameters affecting the temperature distribution in a disc-type transformer winding. *Applied Thermal Engineering*, 30(14-15):2034 – 2044, 2010.

Torriano F., Picher P., and Chaaban M. Numerical investigation of 3d flow and thermal effects in a disc-type transformer winding. *Applied Thermal Engineering*, 40(0):121 – 131, 2012.

Tsili M.A., Amoiralis E.I., Kladas A.G., and Souflaris A.T. Power transformer thermal analysis by using an advanced coupled 3d heat transfer and fluid flow fem model. *International Journal of Thermal Sciences*, 53(0):188 – 201, 2012.